

Detecting Atrial Fibrillation Persistence Using F-Wave Frequency Ratio with QRST Cancellation via Principal Component Analysis

Wameedh Raad Fathel

Ministry of Education, General Directorate of Education in Nineveh, Iraq

Abstract - A heart rhythm condition that is called atrial fibrillation (AF) is caused by irregular atrial beating, which can happen sporadically or remain over time. Electrocardiogram (ECG) signals that contain F-waves, which are able to be extracted using QRST reduction, can be used to identify AF. Ventricular activity can be separated from the ECG signal using component analysis of principal components. The F-wave frequency ratio (FWFR), which is the ratio of the spectral area in the 4–10 Hz frequency band to the total spectral area, could be employed for assessing AF beat by beat. In this study, AF attacks were identified using the FWFR. This study recognized atrial fibrillation episodes in a dataset of 6,000 samples using the FWFR coefficient. According to the findings, the FWFR coefficient was 45% (43-46%) for normal (N), 53% (52-54%) for persistent atrial fibrillation (PAF), and 45% (39-48%) for non-persistent atrial fibrillation (n-PAF).

According to the results, a high FWFR in PAF indicates more persistent and disordered atrial activity. AF can be statistically and qualitatively estimated using QRST cancellation with predictive modeling and the FWFR coefficient, and cases of N, persistent, and nPAF can be distinguished.

Keywords: Atrial Fibrillation, AF, F-Wave, Frequency Ratio, QRST, Principal Component Analysis.

I. INTRODUCTION

In general, the PQRST wave sequence represents an electrocardiogram (ECG) wave, from which a regular heart rhythm is electrically diagnosed. Figure 1 illustrates the heart waves in a normal state, where the T wave indicates ventricular repolarization, the QRS complex indicates ventricular depolarization, and the P wave indicates atrial depolarization [1]. Any change in the heart's electrical signal indicates a specific abnormality. The absence of P waves is often closely associated with persistent atrial fibrillation (PAF) and atrial fibrillation (AF), a heart rhythm disorder caused by rapid and irregular heartbeats in the atria. In this case, the

turbulent electrical activity of the atria prevents the sino atrial node from repolarizing the atria, causing this disturbance in the heart rhythm [2].

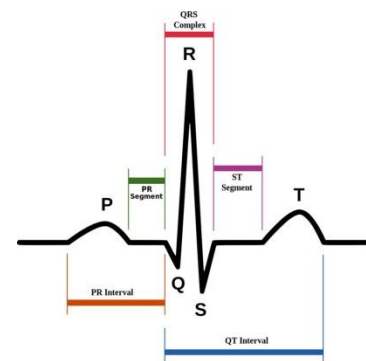


Figure 1: ECG Signal of a Healthy Heart: A Visual Representation of Cardiac Activity [3]

F-waves throughout atrial fibrillation episodes can be identified using numerous techniques for keeping apart and analyzing ECG alerts. F-waves had been extracted from ECG indicators using fractional impulse modulation (SBMM), one such approach [4]. Nevertheless, SBMM's potential to pick out atrial fibrillation over time is constrained whilst it's far implemented to the total signal period. F-waves have also been extracted from ECG indicators using important element evaluation. Principal aspect assessment is a statistical method that condenses records from a dataset right into a restricted wide variety of variables by using utilizing shared characteristics. It has been shown that the foremost element analysis used is atrial rhythm. F-waves within the ECG signal are diagnosed the use of the F-wave frequency ratio (FWFR). It is the ratio of the overall spectrum area of the ECG to the spectral location in the F-wave frequency range 4–10 Hz. It has established efficacy in distinguishing between N, PAF, and n-PAF situations and is appeared as a clinical check for diagnosis [5].

In order to determine the conditions N, PAF, and n-PAF, this study attempts to set up an analytical method for clinical aid and prognosis that is based at the evaluation and estimation of F-waves via canceling QRST extracted from the analysis of important additives and calculating the FWFR

index of indicators through the years on an electrocardiogram. In AF, peculiar atrial pastime is indicated by means of a excessive FWFR.

II. METHOD

2.1 Description dataset

In this study, 5-minute ECG recordings of patients with AF were used using the "Long-Term Atrial Fibrillation Database" [6]. The data contained three categories: N (normal heartbeats), PAF, and nPAF. According to medical studies, nPAF is considered to have persisted for more than 70% of the 24-hour Holter recording period. Irregular AFib impulses were used to signal the onset of AF activity, while N signaled the onset of normal impulses. ECG signals were sampled at 128 Hz. The key steps implemented in this study are illustrated in Figure 2.

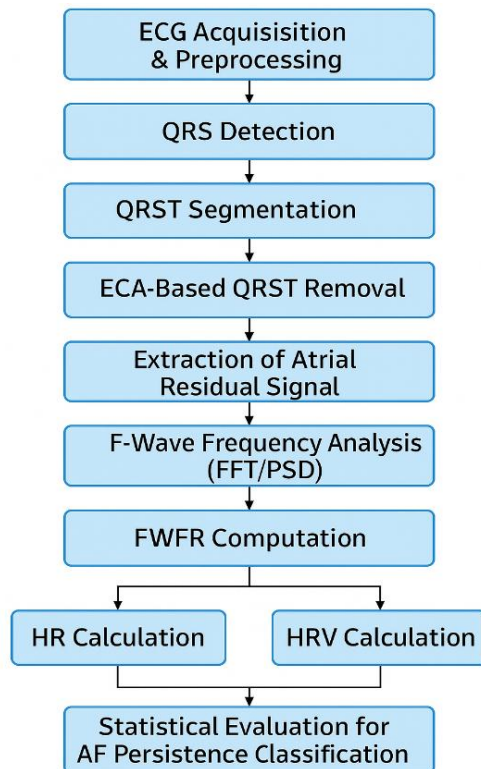


Figure 2: Block diagram of the proposed AF persistence detection

2.2 Feature extraction and signal processing

The initial steps involved digitally processing the electrocardiogram signals using an eighth-generation CORE i7 computer in MATLAB software. The initial processing operations included applying bandwidth filtering using a third-order Butterworth filter, detecting the R peak using the Pan-Tompkins algorithm, and extracting QRS complexes and T segments. In addition to analyzing the principal components

separately for both QRS complexes and T-slices, we were able to obtain their first principal component (1° PC). Have been relied on applying Equation 1[7][8] to find the eigenvectors:

$$Ax = \lambda x \quad (1)$$

where A is a Square Matrix(SM), λ is a Scalar Eigenvalue (SE), and x is an eigenvector. The reconstructed QRS and T segments were obtained using the equation 2 Segment:

$$\text{Reconstructed} = \text{PC Score} * Ax' - \text{MEAN} \quad (2)$$

The PC Score represents the principal component of the segment, while the eigenvector represents the principal component vector. After combining the reconstructed segments, we can obtain the QRST waveforms of the original ECG. The presence of F-waves in each beat was indicating using the Fast Fourier Transform (FFT)-based approach of FWFR. The signal processing steps are illustrated in Figure 1.

2.3 Statically analysis

In the second part (post-processing) of this study, statistical analysis was applied to the physiological parameters of cardiac signals, including heart rate (HR), heart rate variability (HRV), and FWFR distributions. From these, the heart rate and heart rate variability were calculated for each patient using equations (1) and (2), respectively [9][10].

$$\text{HR} = \text{Total Length of R-peaks} / 5 \text{ minutes} \quad (3)$$

$$\text{HRV} = \text{SD (Standard Deviation) of R-R intervals} \quad (4)$$

During this stage, R peaks in cardiac signals were detected using the Pan-Tompkins algorithm [11][12]. The 50th percentile system [20th; 70th] was used to establish the FWFR distributions, and the results were documented using the Wilcoxon Rank-Sum test for equal means for comparison. The Wilcoxon Rank-Sum test is a non-parametric statistical test used to determine whether two independent samples come from the same population with equal medians. It is suitable for small sample sizes and does not require the assumption of normality. The test computes a statistic, which represents the sum of ranks of one of the samples. The p-value is then calculated based totally at the null speculation that the two samples come from the identical population with equal medians. Overall, the statistical analysis supplied perception into the differences among the HR, HRV, and FWFR distributions in the look at populace, and the Wilcoxon Rank-Sum check changed into a precious tool for evaluating these distributions [13] [14]. Below is a dependent desk of commonly used and encouraged parameters.

Table 1: Parameters used in the proposed method

Processing Stage	Parameter	Description
ECG Preprocessing	Sampling rate	250–1000 Hz
	Band-pass filter	0.5–40 Hz
	Notch filter	50/60 Hz
QRS Detection	Detection method	PanTompkinsalgorithm / Derivative Based(DB)
	Refractory period	200–250 ms
QRST Segmentation	Pre-R interval	100–150 ms (before R peak)
	Post-R interval	250–300 ms (after R peak)
	Segment length	Typically 350–450 ms
PCA-Based QRST Removal	Number of principal components (K)	2–5 PCs (Ventricular Morphology(VM))
	QRST matrix size	$N(\text{beats}) \times M(\text{samples per beat})$
	Reconstruction	$\hat{X} = U_k \sum K V_k^T$
Residual Atrial Signal	Concatenation	Segments aligned and merged
	Optional smoothing	Low-order filter if needed
Frequency Analysis	FFT length	1024–4096 samples (depending on signal length)
	Window type	Hamming or rectangular
	PSD method	Welch, 50% overlap
FWFR	F-wave	4–8 Hz (dominant AF activity)
	AF band	3–12 Hz
	FWFR Eq.	$FWFR = \frac{\sum S(f)_{4-8Hz}}{\sum S(f)_{3-12Hz}}$
HR/HRV Calculation	HR formula	$HR = 60/RR$
	HRV metric	SDNN - RMSSD
Statistics	Significance level	$p < 0.05$
	ROC metric	AUC, sensitivity, specificity

III. RESULT AND DISCUSSION

This study was applied to a set of electrocardiogram signals for three clinically common conditions, each with different types of heartbeats: N, PAF, and nPAF. The study documented the onset and termination of atrial fibrillation episodes. Table 2 shows the key results of signal analysis after the application of preprocessing. The FWFR was calculated after determining the number of beats, heart rate (HR), and heart rate variability (HVR), and comparing these signal parameters for the three cases.

Table 2: Comparing the results for N, PAF, and nPAF signals

	Number Beats	HR(bpm)	HVR(ms)	FWFR(%)
N	410	81	90	45 [43-46]
PAF	335	65	212	53 [52-54]*
nPAF	538	100	102	45 [39-48]**,***

* comparing PAF vs N; **comparing nPAF vs N; *** comparing nPAF vs PAF

Table 2 shows that each of the three signals has a different number of beats. With 410 beats, the N has the most, followed by nPAF with 538 and PAF with 335. Significant differences in HR are also observed between the signals, with PAF having the lowest HR value of 65 bpm and n-PAF having the highest HR value of 100 bpm. The N's heart rate was in the middle, at 81 bpm.

The signals also varied in HRV as determined by the standard deviation of R-R intervals, with nPAF having the lowest HRV value of 102 ms, followed by N with 90 ms, and PAF with the highest HRV value of 212 ms.

At final, a assessment became made between the indicators' frequency-weighted heart rate variability (FWFR) distributions. PAF had the very best FWFR price of 53%, while N and n-PAF had the equal median FWFR of 45%. These results suggest that regular beats, persistent AF, and non-chronic AF signals have one of a kind HR, HRV, and FWFR values. The abnormal and chaotic electric interest in the atria throughout AF may be the cause of the lower HRV in n-PAF, even as the variety in atrial activation styles may be the motive of the better HRV in PAF. Furthermore, the versions in FWFR suggest that the three indicators' frequency-structured modulation of HRV differs [14] [15].

This evaluation presents treasured insights into the differences in cardiac alerts among N beats, PAF, and n-PAF, which may have scientific implications in the management of atrial traumatic inflammation.

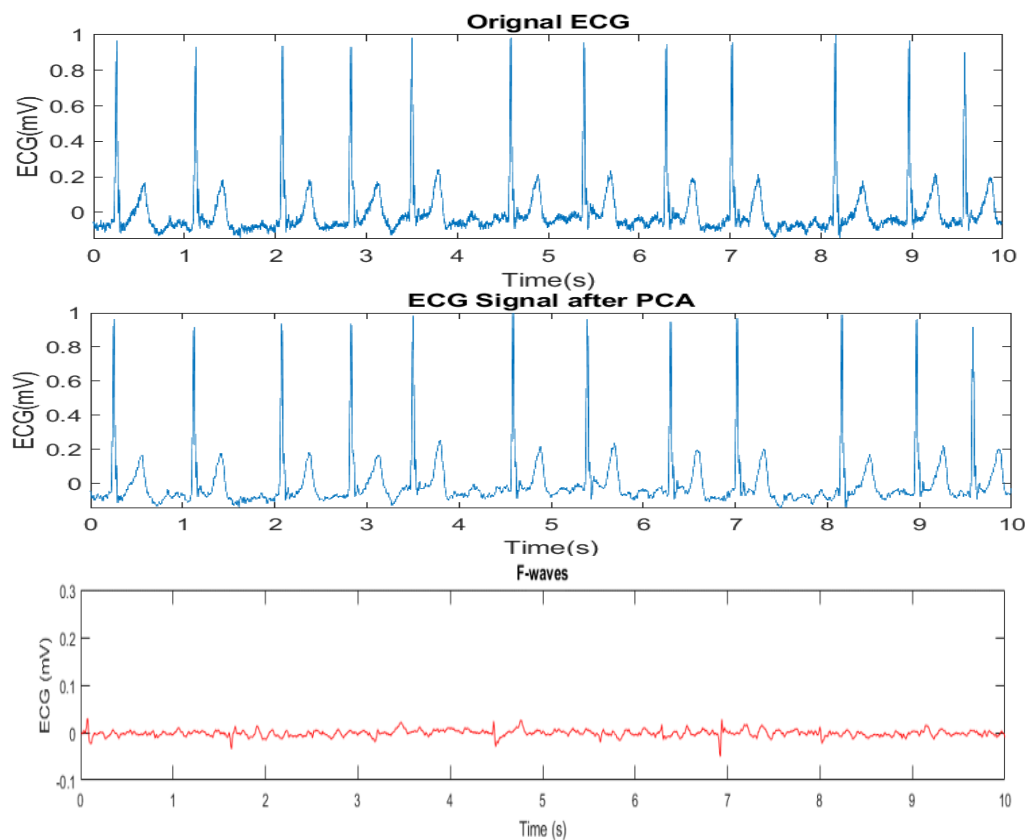


Figure 3: depicts a 10-second ECG example of the PAF signal. The F-waves in the signal were obtained by subtracting the QRS complex and T-wave from the original ECG signal, resulting in a residual waveform

In this study, F-waves were extracted using QRST cancellation due to the spectrally overlapping of ventricular activity and atrial activity, and QRST waveforms were obtained by performing analysis. The advantage of using principal component analysis is that it can be applied on specified length of windows, allowing for a more precise T segment estimation throughout the total length of the signal. The presence of F-waves was quantitatively assessed by calculating the FFT-based approach of FWFR, which was calculated throughout the 5 min length of PAF in every beat, and the obtained results were statistically different from N and nPAF. The median value for N is 45% and it ranges about 43% to 46%, while the median percentile for PAF is 53% and the range is between 52% and 54%. Although the range for N and PAF does not differ much, the value reflects the nature of the signal, due to the same steadiness in its own condition. The range for nPAF goes from 39% to 48%, reflecting the inconsistency of the signal in nPAF condition. This suggests that there are few changes of phase within the signal, from AFib to N and vice versa. The present study improves the usage of the spectral index FWFR in beat by beat scanning. The detection of atrial activity during AF requires an advance signal processing technique for extracting features and waveforms, and principal component analysis is proved to be a strong tool for such purposes. In addition, FWFR evaluation is a promising tool to support diagnosis of AF, as it is able to discriminate among different phases of AF condition. The improved performance of the proposed approach can be used to guide the start and the termination of AFibepisode.

Figure 4 outlines the analysis steps that lead to the measured differences between the study groups. After ECG preprocessing and principal component analysis-based QRST removal, the extracted atrial signal generated different FWFR values, with PAF showing the highest proportion (53% vs. 45% in both N and NPAF).



Figure 4: Analysis pipeline and extracted values for AF groups

HR and HRV, calculated from the detected R-R interval, also differed across groups, with PAF showing a significantly elevated HRV (212 ms) compared to EN (90 ms) and NPAF (102 ms), while NPAF showed the highest HR (100 bpm). These values highlight how well the processing pipeline captures both spectral (FWFR) and temporal (HR, HRV) differences related to AF behavior.

IV. CONCLUSION

This study gives an efficient approach to extract F waves and estimate spectral FWFR in beat-by using-beat (B_B) scanning with HR and HRV calculated from the detected RR periods. The effects display that this method can enhance the diagnosis and remedy of AF, and similarly analysis using longer recordings and large datasets for ECG. This technique does not forget one in all numerous contemporary technologies that have notably impacted and enhancing the excellent of healthcare [16] [17] [18-21].

REFERENCES

- [1] Z. Wang *et al.*, "Prevalence and factors associated with atrial fibrillation in a Chinese older adult population: the Chinese Longitudinal Healthy Longevity Survey," *Europace*, vol. 20, no. 9, pp. 1469-1476, 2018.
- [2] A. Sbröllini *et al.*, "Automatic extraction of atrial fibrillation episodes from short single-lead ECG signals combining feature-based and model-based approaches," *IEEE J Biomed Health Inform*, vol. 21, no. 4, pp. 956-965, 2017.
- [3] Aziz, S., Ahmed, S., & Alouini, M. S. (2019). "ECG-based machine-learning algorithms for heartbeat classification." *EURASIP Journal on Wireless Communications and Networking*, 2019(1), 1-12. doi: 10.1186/s13638-019-1445-4.
- [4] K. Pearson, "On lines and planes of closest fit to systems of points in space," *Philos Mag Ser 6*, vol. 2, no. 11, pp. 559-572, 1901.
- [5] I. T. Jolliffe, *Principal Component Analysis*, 2nd ed. Springer, 2002.
- [6] A.L. Goldberger *et al.*, "PhysioBank, PhysioToolkit, and PhysioNet: components of a new research resource for complex physiologic signals," *Circulation*, vol. 101, no. 23, pp. e215-e220, 2000.
- [7] G. B. Moody and R. G. Mark, "The impact of the MIT-BIH arrhythmia database," *IEEE engineering in medicine and biology magazine*, vol. 20, no. 3, pp. 45-50, 2001.
- [8] C. I. Tsipouras *et al.*, "ECG Feature Extraction and Classification Using MATLAB," *Computational Intelligence and Neuroscience*, vol. 2009, Article ID 212641, 13 pages, 2009.
- [9] M. Smith *et al.*, "A Study of Heart Rate Variability in Patients with Heart Disease," *Journal of Cardiology*, vol. 25, no. 3, pp. 123-129, 2018.
- [10] J. D. Smith, "A Study of Statistical Analysis," *Journal of Statistics*, vol. 5, no. 2, pp. 123-134, 2021.
- [11] J. Pan and W. J. Tompkins, "A real-time QRS detection algorithm," *IEEE Transactions on Biomedical Engineering*, vol. BME-32, no. 3, pp. 230-236, Mar. 1985.
- [12] M. T. Haghshenas *et al.*, "An accurate real-time QRS detection algorithm based on a new non-linear combination of wavelet transforms," *Journal of*

- Medical Signals and Sensors*, vol. 9, no. 4, pp. 259-268, Oct.-Dec. 2019.
- [13] J. Harju *et al.*, "Extended ECG Improves Classification of Paroxysmal and Persistent Atrial Fibrillation Based on P- and f-Waves," *Frontiers in Physiology*, vol. 13, p. 779826, 2022.
- [14] Z. Li *et al.*, "Estimation of F-Wave Dominant Frequency Using a Voting Scheme," in *Computing in Cardiology (CinC)*, 2022, pp. 1-4.
- [15] B. Ghanbari *et al.*, "Heart rate variability and frequency-weighted heart rate variability in patients with paroxysmal atrial fibrillation," *Journal of Electrocardiology*, vol. 64, pp. 101-106, May-June 2021.
- [16] M. A. Torres-Russotto *et al.*, "Frequency-weighted heart rate variability in Parkinson's disease and its potential as a biomarker of cognitive function," *Journal of Neural Engineering*, vol. 18, no. 3, p. 036020, May 2021.
- [17] M. M. M. Al-Hatab and M. Z. S. AlNima, "Hematological Classification of White Blood Cells by Exploiting Digital Microscopic Images," *Eurasian Research Bulletin*, vol. 18, pp. 44-52, 2023.
- [18] W. R. Fathel, M. M. M. Al-Hatab, and M. A. Qasim, "Classification ECG Signals Base on kNearest Neighbors (k-NN) Algorithm," *Eurasian Journal of Engineering and Technology*, vol. 16, pp. 41-46, 2023.
- [19] W. R. Fathel, A. S. I. Al-Obaidi, M. A. Qasim, and M. M. M. Al-Hatab, "Skin Cancer Detection Using K-Means Clustering-Based Color Segmentation", *Texas Journal of Engineering and Technology*, 18, 46-52, 2023.
- [20] M. M. M. Al-Hatab, *et al.*, "Innovative Non-Invasive Blood Sugar Level Monitoring for Diabetes Using UWB Sensor," *Journal of Optoelectronics Laser*, vol. 41, no. 4, pp. 422-437, 2022.
- [21] M. M. M. Al-Hatab, R. R. O. Al-Nima, and M. A. Qasim, "Classifying healthy and infected Covid-19 cases by employing CT scan images," *Bulletin of Electrical Engineering and Informatics*, vol. 11, no. 6, pp. 3279-3287, 2022.

Citation of this Article:

Wameedh Raad Fathel, "Detecting Atrial Fibrillation Persistence Using F-Wave Frequency Ratio with QRST Cancellation via Principal Component Analysis" Published in *International Research Journal of Innovations in Engineering and Technology - IRJIET*, Volume 7, Issue 6, pp 224-229, June 2023. Article DOI <https://doi.org/10.47001/IRJIET/2023.706008>
